ORIGINAL RESEARCH

# Role of MicroRNA-150 and Glycoprotein Nonmetastatic Melanoma Protein B in Angiogenesis during Hyperoxia-Induced Neonatal Lung Injury

Telugu Narasaraju*, Dhananjay Shukla*, Sunil More, Chaoqun Huang, Li Zhang, Xiao Xiao, and Lin Liu

The Lundberg-Kienlen Lung Biology and Toxicology Laboratory, Department of Physiological Sciences, Center for Veterinary Health Sciences, Oklahoma State University, Stillwater, Oklahoma

## Abstract

Glycoprotein nonmetastatic melanoma protein B (GPNMB), a transmembrane protein, has been reported to have an important role in tissue repair and angiogenesis. Recently, we have demonstrated that hyperoxia exposure down-regulates microRNA (miR)-150 expression and concurrent induction of its target gene, GPNMB, in neonatal rat lungs. This study aimed to test the hypothesis that soluble GPNMB (sGPNMB) promotes angiogenesis in the hyperoxic neonatal lungs. Wild-type (WT) or miR-150 knockout (KO) neonates, exposed to 95% $O_2$ for 3, 6, and 10 days, were evaluated for lung phenotypes, GPNMB protein expression in the lungs, and sGPNMB levels in the bronchoalveolar lavage. Angiogenic effects of sGPNMB were examined both *in vitro* and *in vivo*. After a 6-day exposure, similar analyses were performed in WT and miR-150 KO neonates during recovery at 7, 14, and 21 days. miR-150 KO neonates displayed an increased capillary network, decreased inflammation, and less alveolar damage compared with WT neonates after hyperoxia exposure. The early induction of GPNMB and sGPNMB were found in miR-150 KO neonates. The recombinant GPNMB, which contained a soluble portion of GPNMB, promoted endothelial tube formation *in vitro* and enhanced angiogenesis *in vivo*. The increased capillaries in the hyperoxic lungs of miR-150 KO neonates appeared dysmorphic. They were abnormally enlarged in size and occasionally laid at subepithelial regions in the alveoli. However, the lung architecture returned to normal during recovery, suggesting that abnormal vascularity during hyperoxia does not affect postnatal lung development. GPNMB plays an important role in angiogenesis during hyperoxia injury. Treatment with GPNMB may offer a novel therapeutic approach in reducing pathologic complications in bronchopulmonary dysplasia.

**Keywords:** microRNA-150; bronchopulmonary dysplasia; glycoprotein nonmetastatic melanoma protein B; angiogenesis

### Clinical Relevance

This study suggests an important role of glycoprotein nonmetastatic melanoma protein B (GPNMB). Targeting GPNMB may provide a therapeutic approach for treating bronchopulmonary dysplasia.

Preterm newborns, with low birth weights (<1,000 g), are at high risk for the development of bronchopulmonary dysplasia (BPD) due to surfactant deficiency, ventilation therapy (barotrauma or volutrauma), maternal infections, and supplemented oxygen toxicity (1–3). These factors contribute to severe lung injury with atelectasis, impaired capillaries, and alveolar development (4–6). Improvements in patient care and ventilation strategies significantly increase the survival of extremely premature babies. However, these infants develop lung abnormalities, clinically known as "new BPD," with characteristic lesions of enlarged alveoli and impaired capillary formation (7–9). An estimated affliction of 10,000–15,000

(Received in original form January 15, 2013; accepted in final form July 14, 2014)

*These authors contributed equally to this work.

This work was supported by National Institutes of Health grants R21HL087884 and R01HL116876, and by Oklahoma Center for the Advancement of Science and Technology grant HR08-064 (L.L.).

Correspondence and requests for reprints should be addressed to Lin Liu, Ph.D., Department of Physiological Sciences, Oklahoma State University, 264 McElroy Hall, Stillwater, OK 74078. E-mail: lin.liu@okstate.edu

This article has an online supplement, which is accessible from this issue's table of contents at www.atsjournals.org

Am J Respir Cell Mol Biol Vol 52, Iss 2, pp 253–261, Feb 2015

Originally Published in Press as DOI: 10.1165/rcmb.2013-0021OC on July 23, 2014
Internet address: www.atsjournals.org

infants with BPD is reported every year in the United States (10), and accounts for 85% of all preterm complications. Due to lung damage at early developmental stages, these patients suffer with persistent respiratory complications beyond their childhood (11, 12). A better understanding of the molecular events leading to these complications is essential in developing new therapeutic treatments to reduce pathological lesions of new BPD cases.

Impairment of angiogenesis results in alveolar arrest, whereas promoting angiogenesis improves alveolar growth and lung functions (13–15). During alveolarization, the capillary endothelial cells play an essential role in the formation of secondary septae. This is described as a "vascular hypothesis" (16–18). Orchestration of these morphologic changes is regulated by various signaling pathways and growth factors (19–21). The vascular endothelial growth factor (VEGF) is the key angiogenic growth factor, but other growth factors, such as angiopoietin-1, are also known to have a role in angiogenesis (22). Animal and human studies have demonstrated that VEGF is down-regulated during BPD (23, 24). Therapeutic treatment or restoration, through VEGF gene transfer, ameliorates lung injury, suggesting that manipulating angiogenesis may have a therapeutic value in treating preterm infants (18, 24, 25). Interestingly, preterm infants exposed to a longer period of ventilation showed increased abnormal vascularity, due to the increased angiogenic factor, endoglin, a glycoprotein that regulates transforming growth factor-β receptor complex (26). These results highlight the existence of alternative angiogenic factors, which could have a potential role in compensating the loss of VEGF in promoting angiogenesis.

MicroRNAs (miRNAs) are small, noncoding RNAs, and are implicated in diverse biological processes and diseases (27–29). Recent studies support the direct link between miRNAs and angiogenesis, including endothelial migration, proliferation, and vessel formation (30–33). The involvement of miRNAs in embryonic lung development is well documented, but their role in BPD is largely unexplored. We have recently identified several miRNAs significantly altered in hyperoxia-exposed rat neonatal lungs (34). One of the down-regulated miRNAs, miR-150, has several angiogenic factors as targets, including glycoprotein nonmetastatic melanoma protein B (GPNMB). GPNMB is a transmembrane glycoprotein, also known as osteoactivin, and is involved in the differentiation of osteoblasts and angiogenesis (35, 36). GPNMB contains an arginine-glycine-aspartic acid (RGD) domain and two heparin binding domains in the extracellular region of the protein. The RGD domain binds to $\alpha_v\beta_3$ integrin receptors on endothelial cells and promotes their migration and proliferation (37).

In the present study, we tested the hypothesis that soluble GPNMB (sGPNMB) promotes angiogenesis in the hyperoxic neonatal lungs. We evaluated the role of miR-150 and GPNMB in angiogenesis and morphogenesis in neonatal lungs during hyperoxia-induced injury using miR-150 knockout (KO) neonates. miR-150 KO mice showed an increase in angiogenesis and a decrease in inflammation in the lungs when exposed to hyperoxia compared with wild-type (WT) neonates. An early induction of GPNMB and an increased release of sGPNMB in the hyperoxic lungs of miR-150 KO mice were also observed. Furthermore, a soluble portion of GPNMB promoted angiogenesis, both *in vitro* and *in vivo*. Although increased vascularity in miR-150 KO neonates appeared dysmorphic, by which they were abnormally enlarged in size and occasionally laid at subepithelial regions in the alveoli, these abnormalities did not affect the later stages of lung development. miR-150 KO neonates had normal lung architecture during recovery, and, remarkably, miR-150 KO neonates recovered faster than the WT counterparts, indicating that the appearance of abnormal vasculature during hyperoxia injury is transient. Taken together, these data suggest a novel role of miR-150 and its target gene, GPNMB, in angiogenesis, during hyperoxia-mediated lung injury.

## Materials and Methods

### Animals

All animal procedures were performed according to the protocol approved by the

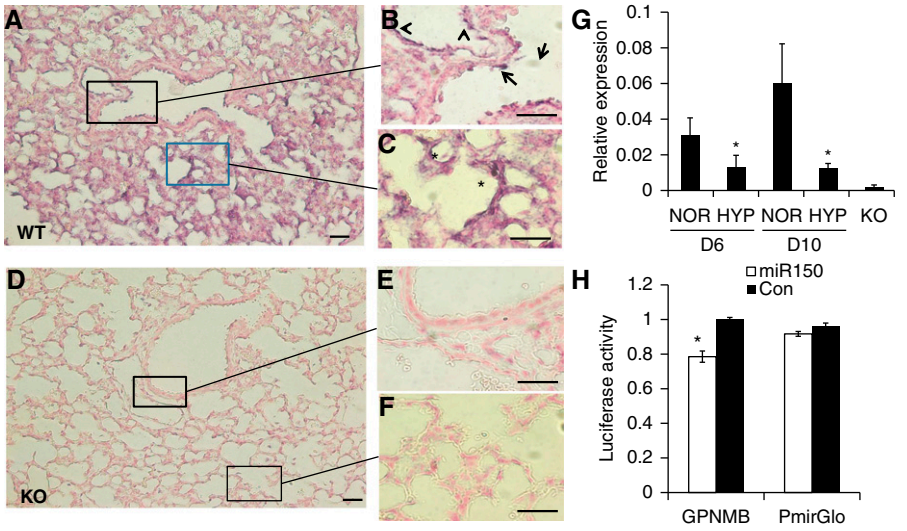


**Figure 1.** Expression of microRNA (miR)-150 in the lungs. (*A–C*) *In situ* hybridization was performed to evaluate cellular expression of miR-150 in wild-type (WT) and miR-150 knockout (KO) neonatal mouse lungs. The lung sections were hybridized with a 5′- and 3′-digoxigenin–labeled locked nucleic acid probe against miR-150. Positive signals were visualized as *dark blue/purple staining*. *Arrows* denote signals from bronchiolar epithelia; *arrowheads* indicate staining in endothelial cells; and *asterisks* indicate miR-150 expression in alveolar epithelial cells. (*D–F*) No staining was detected in miR-150 KO neonatal mouse lungs. *Scale bars*, 40 μm. (*G*) Quantitative real-time PCR was performed to evaluate the expression of miR-150 during hyperoxia injury. Values were expressed as means ± SE from four neonatal mouse pups. D6 and D10, exposures for 6 and 10 days; HYP, hyperoxia; NOR, normoxia. (*H*) Glycoprotein nonmetastatic melanoma protein B (GPNMB) 3′-untranslated region (UTR) reporter assay. Human embryonic kidney 293T cells were cotransfected with a 3′-UTR reporter vector together with an miR-150 expression vector or a control vector (Con), and dual luciferase assays were performed. PmirGlo without 3′-UTR insert was used as a negative control ($n$ = 3 independent experiments). *$P < 0.05$ versus Con.

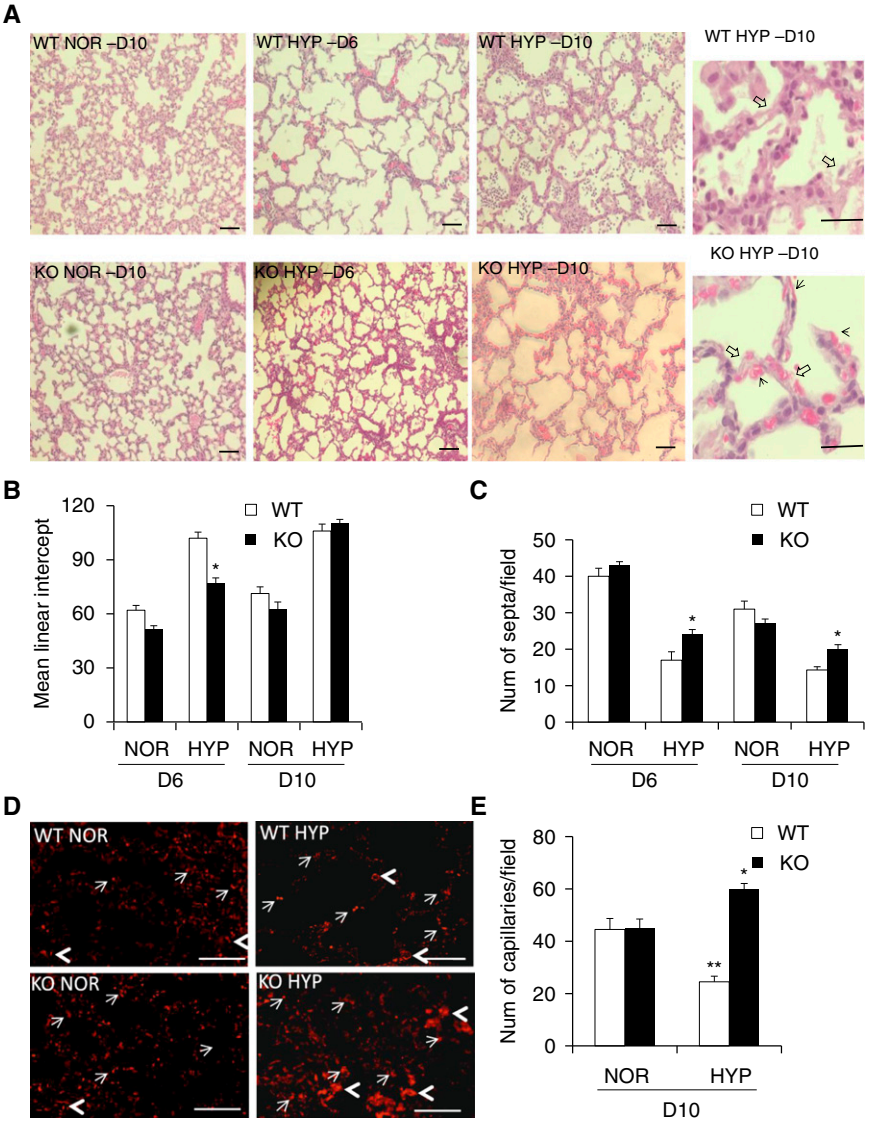


**Figure 2.** Phenotypic differences in the lungs between miR-150 KO and WT mice after exposure to hyperoxia. (*A*) The 3-day-old WT and miR-150 KO mouse pups were exposed to 95% $O_2$ for 6 and 10 days. Lungs were fixed and stained with hematoxylin and eosin. No difference in the lung architecture was found in room air–exposed WT and miR-150 KO neonates. At 6 days of exposure, WT neonates showed enlarged alveoli compared with miR-150 KO neonates. By 10 days of exposure, significant increases in alveolar size were noted in both WT and miR150 KO neonates. However, WT neonates displayed mild to moderate inflammation in the lungs, whereas miR-150 neonatal lungs showed little inflammation. Mild to moderate inflammation is defined based on the overall distribution of inflammatory cells in the alveolar airspace. In mild inflammation, cells are focally distributed, and the numbers are less and have occasional appearances of neutrophils. Moderate inflammation represents increased and frequent neutrophilic infiltrations, whereas severe inflammation is wide spread, with high neutrophil and macrophage infiltration in the alveolar air space. KO, miR-150 KO. *Arrowhead*, capillaries in alveoli; *open arrows*, alveolar epithelial damage. (*B*) Mean lineal intercept (MLI) values. The MLI was determined by dividing the length of lines across an image field by the total number of alveolar intercepts from 25 lines from each lung section. Data shown are means ± SE ($n = 3$). (*C*) Secondary septa formation was measured by counting the number of septal sproutings in a minimum of 5–10 fields of each sample ($n = 3$). Secondary septa were identified from nonoverlapping alveolar regions. Sprouting branches that emerge from existing alveoli and are not interconnected were counted. Growing septa also contains a distinct outer capillary layer. (*D*) Capillary network formation determined by platelet/endothelial cell adhesion molecule 1 (PECAM1) immunostaining. *Arrows*, capillaries within the septa; *arrowheads*, endothelial staining in large blood vessels. (*E*) Quantitative analysis of capillary numbers within the alveolar septa measured from 400× images from D10-exposed lungs ($n = 3$). *Scale bars*, 40 μm. *$P < 0.05$ versus WT HYP; **$P < 0.05$ versus WT NOR.

Animal Care and Use Committee (protocol no. VM1025) at Oklahoma State University. The breeding pair of WT (C57BL/6J) and miR-150 KO (B6(C)-*Mir150*$^{tm1Rsky}$/J) mice were purchased from The Jackson Laboratory (Bar Harbor, ME). Both the WT and miR-150 KO mice were bred in-house.

### Exposure of Neonatal Mouse Pups to Hyperoxia

The neonatal mouse pups from three mothers, delivered on the same day, were mixed and divided into two groups. On Postnatal Day 3 (P3), one group of pups was placed in a sealed Plexiglas chamber (90 × 45 × 45 cm) and exposed to 95% $O_2$ for 3 (D3), 6 (D6), and 10 days (D10), while the other group was kept in room air (34). The mother dams were switched between litters daily. The oxygen flow rate was maintained at 4 L/min and monitored with an oxygen sensor (Vacu-Med, Ventura, CA). In another study, WT and miR-150 KO neonates were exposed to 95% $O_2$ for 6 days and allowed to recover in room air for 7, 14, and 21 days.

### Tissue Collection

At each time point, neonatal pups were anesthetized, trachea cannulated, and had their lungs fixed with 4% paraformaldehyde by instilling endotracheally at a 30-cm $H_2O$ pressure. For RNA and protein samples, the lungs were excised and immediately frozen in liquid nitrogen until further use. For the bronchoalveolar lavage (BAL) collection, neonatal pups were lavaged with 200 μl of PBS twice, with a 27 gauge syringe needle. More than 90% of lavaged fluid was recovered from the neonatal pups. BAL fluids were centrifuged at 1,100 × *g* for 10 minutes and the supernatants were stored at −80°C until further use.

### Expression of miR-150 in the Lungs

Real-time PCR was performed to evaluate the expression of miR-150 during hyperoxia exposure by using miR-150–specific primers as described previously (34). *In situ* hybridization was performed to identify cell-specific expression of miR-150 in the lungs, with 5′- and 3′-digoxigenin–labeled locked nucleic acid probes (Exiqon, Woburn, MA) as described previously (38).

### 3′-Untranslated Region Reporter Assay

3′-Untranslated region (UTR) reporter assay was performed to determine whether

miR-150 binds the 3′-UTR of GPNMB as described previously (34). 3′-UTR encompassing two putative miR-150 binding sites of GPNMB was amplified from mouse lung genomic DNA (BioChain Institute, Newark, CA) using GPNMB-UTR primers (forward, 5′-TATCTCGAGACTC TTCTGTGCATGTATGTGA-3′, and reverse, 5′-ACATCTAGACCTAGAAAT AAGCAATTCCTGG-3′). The PCR fragment was inserted into the downstream of the pmirGLO vector (Promega, Madison, WI). This vector also contains *Renilla* luciferase as a control. For a dual-luciferase assay, human embryonic kidney 293T cells were transfected with an miR-150 expression vector and a 3′-UTR reporter vector using Lipofectamine 2000 (Invitrogen, Carlsbad, CA). Firefly and *Renilla* luciferase activities were measured using the Dual-Luciferase Reporter Assay System (Promega) and FLUOstar Optima (BMG Labtech Inc., Cary, NC).

### Other Methods

Lung histopathology, morphometric analyses, terminal deoxynucleotidyl transferase dUTP nick end labeling (TUNEL) assay, Western blot analysis, ELISA, *in vitro* and *in vivo* angiogenesis assays, and GPNMB expression are described in the online supplement.

### Statistical Analysis

All of the data have been expressed as mean (± SE). For statistical analyses, which were performed with a Student's *t* test, a *P* value of less than 0.05 was considered significant.

## Results

### miR-150 Is Highly Expressed in the Neonatal Lungs and Decreased in Response to Hyperoxia

Expression of miR-150 in the lungs was evaluated by *in situ* hybridization. miR-150 was detected in WT neonatal mouse lungs (Figures 1A–1C), but not in miR-150 KO neonates (Figures 1D–1F). Staining was prominent in the bronchiolar and alveolar epithelial cells (Figures 1B and 1C), and focal staining of miR-150 was also found in the endothelial cells (Figure 1B). The exposure of neonatal mouse pups to hyperoxia down-regulated the expression of miR-150 by more than 50 and 75% at 6 and 10 days of exposure, respectively (Figure 1G). These results are in concurrence with our previous findings in neonatal rat pups (34).

### GPNMB Is the Target of miR-150

We performed a 3′-UTR reporter assay to determine whether miR-150 binds the 3′-UTR of the mouse GPNMB gene. We cloned the 3′-UTR region of mouse GPNMB into the upstream of firefly luciferase using a pmirGLO vector. As shown in Figure 1H, a decrease in luciferase activity was found in the cells transfected with a miR-150 expression vector compared with the cells transfected with the vector control. miR-150 had no effects on the empty vector, pmiRGLO. This result confirmed our previous findings that GPNMB is the target of miR-150 in neonatal rats (34).

### Neonatal Mouse Pups Lacking miR-150 Are More Resistant to Hyperoxia-Induced Damage and Display a Reduced Inflammation Compared with WT Pups

miR-150 KO mice are viable, fertile, and morphologically normal (39). We also did not observe any differences in gestation time or litter size between WT and miR-150 KO mice. There were no differences in lung histology and alveolar development between WT and KO neonates exposed to room air for 3, 6, and 10 days. At 3 days of exposure, no prominent damage was observed in either WT and KO neonatal mice (data not shown). In contrast, at 6 days of exposure, WT mice displayed enlarged alveoli compared with KO neonates (Figure 2A), as is evident by the higher MLI values in WT neonates (Figure 2B). At 10 days of exposure, no significant differences in MLI values were noted between WT and KO neonatal mice (Figure 2B). The secondary septa formation was increased in KO neonates compared with WT pups (Figure 2C). Increased capillaries in KO neonates were more prominent in proximal airways compared with distal airways after hyperoxia exposure. Quantification of capillaries by platelet/endothelial cell adhesion molecule 1 (PECAM1, or CD31) staining confirmed high vasculature in the hyperoxia-exposed KO neonates (Figures 2D and 2E). There was no inflammation observed in both WT and KO neonates until 6 days of exposure.

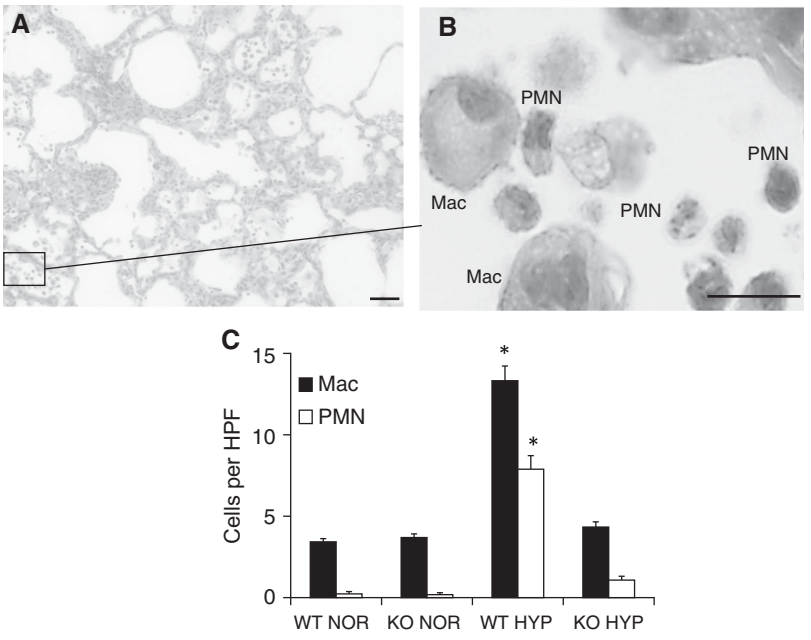


**Figure 3.** Hyperoxia-induced inflammation in neonatal lungs. Hematoxylin and eosin lung sections from WT and KO neonates at 10 days of hyperoxia exposure were evaluated for inflammation in the lungs. Macrophages (Mac) and neutrophils (PMN) were identified in hematoxylin and eosin–stained lung sections by their morphology at high magnification. (*A* and *B*) Representative images of macrophages and neutrophils at low and high magnification. (*C*) Quantitative analysis of macrophages and neutrophils were determined and at least 20 fields were used for cell counting. Values are mean ± SE per high-power field (HPF; 400×; $n = 3$ in each group). *Scale bars*, 40 μm. *$P < 0.05$ versus KO group.

Significant increases in inflammatory cellular infiltrates, including macrophages and neutrophils, were observed in WT neonates compared with KO neonates at 10 days of exposure (Figures 3A–3C).

Alveolar epithelial damage was assessed by TUNEL assay. We quantified TUNEL-positive epithelial cells within the alveolar lining. As shown in Figure 4, a significant increase in alveolar epithelial apoptosis was observed in WT neonatal mice compared with KO mice. These results are consistent with the histopathology analysis, which showed increased alveolar epithelial disruption in WT neonates compared with KO neonates.

### Absence of miR-150 Causes Early Up-Regulation of GPNMB and Release of sGPNMB upon Hyperoxia Exposure

To evaluate whether lack of miR-150 influences GPNMB expression during hyperoxia-exposure, we determined lung GPNMB levels and measured the release of sGPNMB. There was no difference in basal lung GPNMB levels in WT and KO neonates. However, a significant induction of GPNMB was observed in KO neonates compared with WT neonates at 6 days of exposure. At 10 days of exposure, both WT and KO neonates showed an increase in GPNMB levels (Figures 5A and 5B). Similarly, we found an increased release of sGPNMB in BAL fluids of KO neonates at 6 days of exposure compared with their WT counterparts (Figure 5C).

A recent study has shown that intraocular injection of pre–miR-150 reduces VEGF expression (30). We thus examined VEGF protein levels in the lungs of WT and miR-150 KO neonates. As shown in Figures 5D and 5E, the expression of VEGF decreased in both WT and KO neonates after a 10-day hyperoxia exposure compared with their basal expression levels. However, there were no significant differences in VEGF levels under basal or hyperoxic conditions between the WT and miR-150 KO mice.

### Extracellular Domain of GPNMB Induces Endothelial Tube Formation, Migration, and *In Vivo* Angiogenesis

The concentrations of sGPNMB detected in the BAL fluids were 2–8 ng/ml, which are very low for angiogenesis assays *in vitro*. Hence, we used recombinant human GPNMB (rhGPNMB) to examine endothelial tube formation using an *in vitro* angiogenesis kit, endothelial migration using a scratch assay, and *in vivo* angiogenic activity using a matrigel plug assay. As shown in Figures 6A and 6B, incubation with rhGPNMB showed a concentration-dependent increase in tube formation, measured as the number of tube-forming cells per field. rhGPNMB at 250 ng/ml showed a comparable result with VEGF and a complete medium containing growth factors for tube formation. Similarly, rhGPNMB also induced endothelial migration, as evident by enhanced wound healing, which was inhibited by anti-GPNMB antibodies (Figure 6C). The use of a matrigel plug, supplemented with recombinant GPNMB, showed a significant increase in blood vessels (Figure 7). These results suggest that GPNMB could promote angiogenesis by increasing endothelial migration and tube formation.

### miR-150 KO Neonates Display Normal Vascular and Alveolar Repair during Recovery

Recent studies have identified abnormal microvasculature in preterm infants during long-term ventilation (26). Likewise, we observed an increased vascularity in KO neonates, which often showed a pattern of dysmorphic capillaries with abnormally enlarged size and/or lying below the alveolar epithelium (*see* Figures E1A–E1C in the online supplement). The abnormal vasculature was rarely observed in WT neonates (Figures E1D and E1E). To determine whether this abnormality affects the post-hyperoxia lung development, we allowed the animals to recover in room air for 7, 14, and 21 days after a 6-day exposure and performed morphometry analysis and capillary counts. On Day 7 of recovery, both WT and miR-150 KO neonates showed an increase in cellularity and interstitial thickness (Figure E2A), with predominant alveolar epithelial hyperplasia. Although there was an increase in cellularity in the alveoli, WT neonates showed higher MLI values compared with KO neonates (Figure E2B). Capillaries appeared normal in size and shape in KO neonates, which had dysmorphic vasculature during hyperoxia exposure. The capillary numbers in WT neonates were lower compared with KO neonates on Day 7 of recovery (Figure E2C). In addition, immunostaining showed more GPNMB-positive cells in KO neonates compared with WT neonates on Day 7 of recovery (Figure E2D). The proliferative histology and alveolar hyperplasia were subsided on Day 14 of recovery, and both groups of animals showed normal alveolar architecture. Similarly, no differences were found in MLI values or capillary numbers in both WT and KO neonates. These results indicate that miR-150 KO animals recover faster than WT neonates. The vascular abnormalities found during

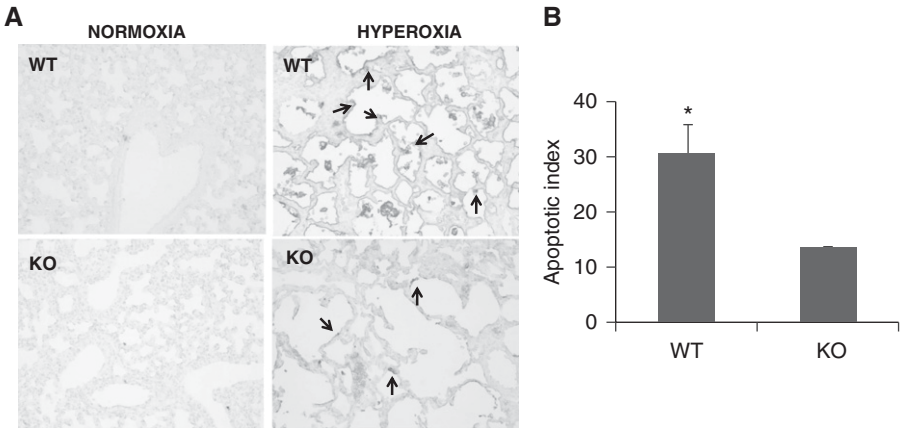


**Figure 4.** Detection of apoptosis in the lungs. Terminal deoxynucleotidyl transferase dUTP nick end labeling (TUNEL) assay was performed in lung sections from WT and miR-150 KO neonatal mouse pups exposed to hyperoxia for 10 days. (*A*) Representative micrographs depicting the lungs of WT and miR-150 KO that were exposed to normoxia or hyperoxia. *Arrows* indicate the apoptotic positive epithelial cells within the alveolar lining. (*B*) Quantification of apoptosis was determined by the number of positively stained alveolar epithelial cells. The apoptotic index indicates the percentage of TUNEL-positive alveolar epithelial cells in the total cells in the field, and the results are expressed as means ± SE ($n$ = 3 animals). *$P < 0.05$ versus miR-150 KO.

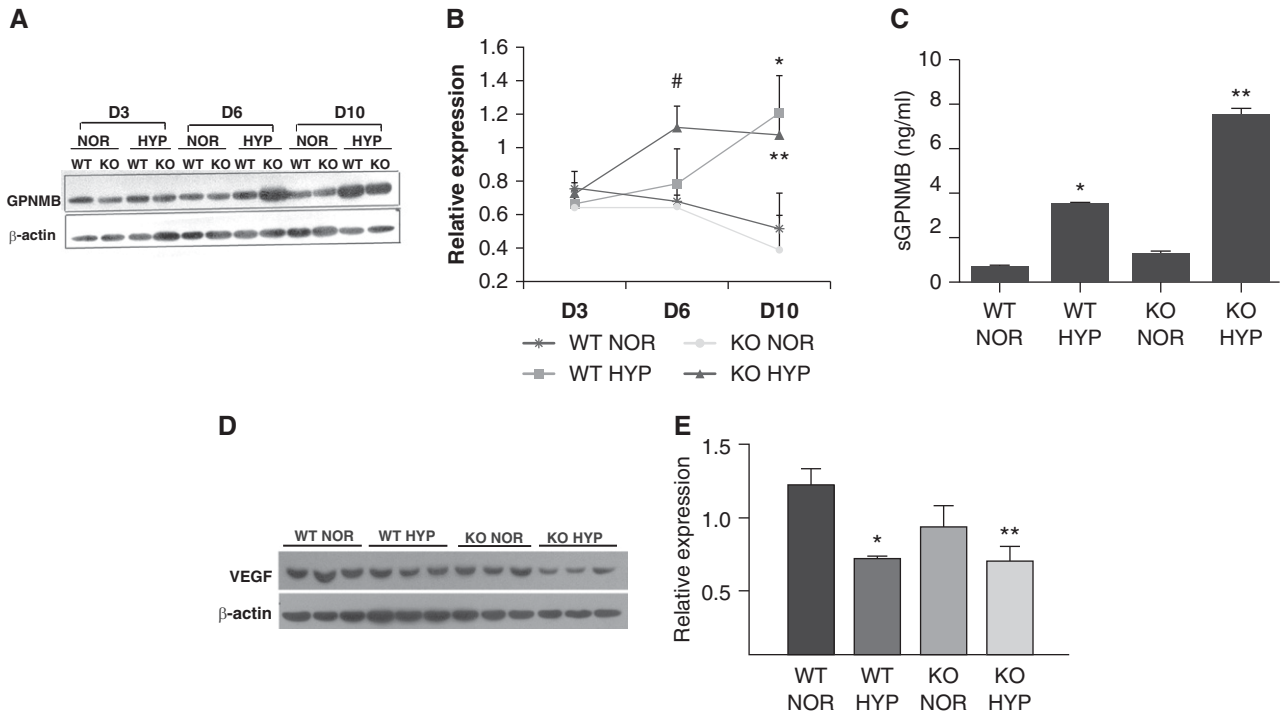


**Figure 5.** GPNMB expression and soluble GPNMB (sGPNMB) levels in the lungs. (*A*) Western blot analysis of GPNMB in the lung homogenates from WT and miR-150 KO neonatal mice after 95% $O_2$ exposure for 3, 6, and 10 days (D3, D6, and D10, respectively). (*B*) Quantitative analysis of GPNMB expression in the lungs showed a significant increase in GPNMB levels in miR-150 KO neonates at D6 and in both WT and miR-150 KO neonates at D10 after hyperoxia exposure. (*C*) sGPNMB levels in the bronchoalveolar lavage (BAL) fluids from air- or hyperoxia-exposed lungs of WT and miR-150 at D6 were analyzed by ELISA. sGPNMB levels were normalized to urea. (*D*) Expression of VEGF in the lungs of WT and miR-150 KO neonates. (*E*) Quantitative analysis of VEGF in the lungs of WT and miR-150 neonates ($n$ = 4–6). $^{\#}P < 0.05$ versus WT HYP; $^{*}P < 0.05$ versus WT NOR; $^{**}P < 0.05$ versus KO NOR.

hyperoxia exposure in the KO neonates disappeared during recovery, suggesting that these abnormalities are transient and preserve normal lung growth during recovery. We did not find any abnormal repair or fibrotic changes in either WT or KO neonates during recovery, as evaluated by staining with Verhoeff Van Gieson and Picro-Sirius red. Both WT and KO neonate lungs appeared normal on Day 21 of recovery (data not shown).

## Discussion

Previous studies have shown that GPNMB enhances tissue repair by inducing autophagy and also promotes angiogenesis during tumor growth (36, 37, 40). We have recently identified GPNMB as one of the targets for miR-150 (34). In the current study, we used miR-150 KO neonatal mice to determine the role of miR-150 and GPNMB in angiogenesis during hyperoxia injury. Hyperoxia exposure induced a significant up-regulation of GPNMB and release of sGPNMB into the alveolar airspace in miR-150 KO at earlier time points compared with that of WT neonates. Hyperoxia exposure impaired vascular growth and increased cellular infiltrates in WT neonates. In contrast, miR-150 KO neonates displayed increased vascularity and minimal inflammation. Recombinant GPNMB, containing a soluble portion of the protein, induced endothelial tube formation and promoted *in vivo* blood vessel formation. Notably, increased pulmonary vasculature in miR-150 KO neonates often appeared dysmorphic, with abnormally enlarged capillaries, which occasionally laid at subepithelial regions in the alveoli. These vascular abnormalities disappeared during recovery in room air, suggesting that these pathologic changes are transient and do not persist in post-hyperoxia lung development. Moreover, miR-150 KO neonates with abnormal vasculature displayed a fast recovery. Taken together, these studies demonstrate the role of miR-150 and its target, GPNMB, in lung vascular growth, which is a possible mechanism to overcome the loss of VEGF during hyperoxia exposure in neonatal mouse pups.

Our previous studies have shown that GPNMB is a target of miR-150 in rats (34). We have confirmed this finding in mice using 3′-UTR reporter assay in the current study. Surprisingly, the expression of GPNMB at basal levels did not show any differences in the lungs between miR-150 KO and WT neonates. The reasons for this discrepancy need further investigation. One possibility is that GPNMB is regulated by miR-150 only under hyperoxic conditions through an unknown mechanism. For example, miR-150 may only regulate GPNMB expression when one or more factors are induced by hyperoxia. Although miR-150 levels were decreased in WT neonates during hyperoxia exposure, there was still roughly 40% of miR-150 remaining at 6 days of exposure, which could account for a lack of induction of GPNMB in the WT neonates on this day. In contrast, GPNMB induction in KO neonates was found at 6 days of exposure, possibly due to the absence of miR-150.

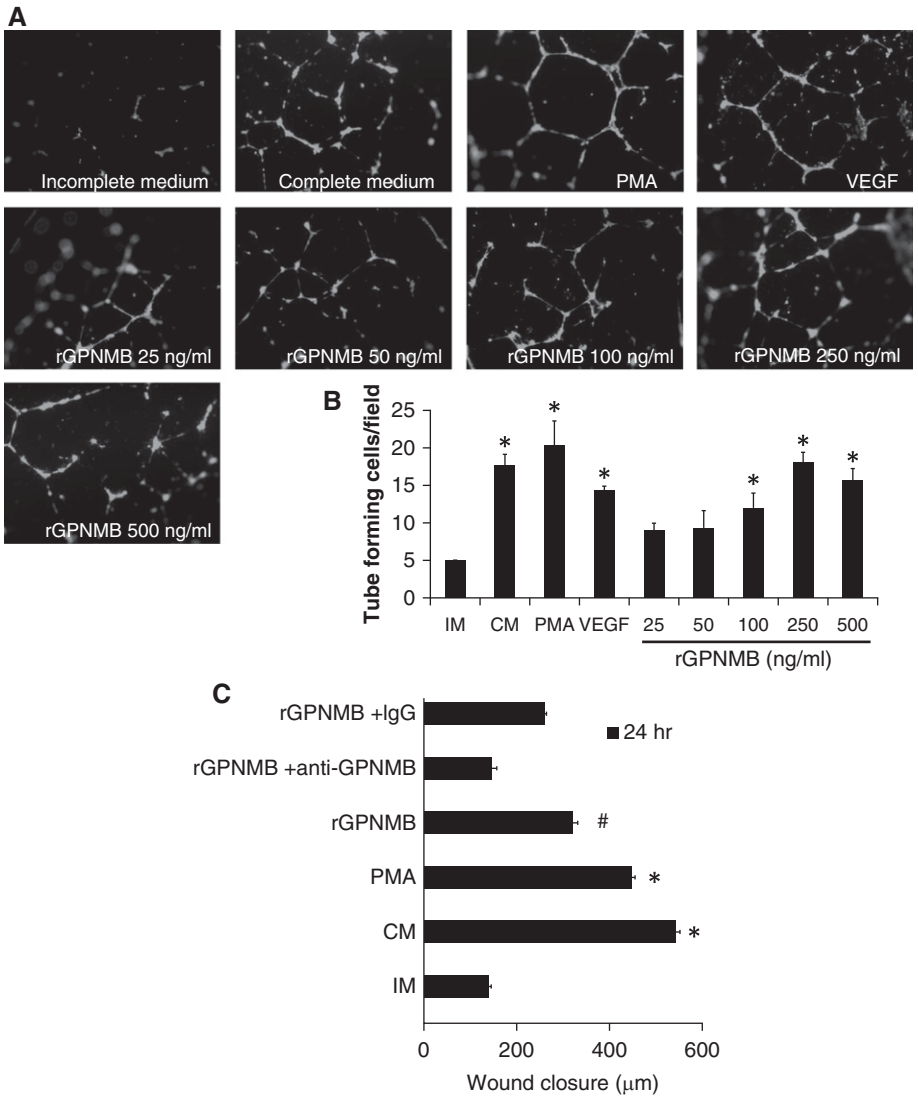


**Figure 6.** *In vitro* angiogenesis and endothelial cell migration induced by recombinant GPNMB (rGPNMB). (*A*) *In vitro* angiogenesis assay. Human umbilical vein endothelial cells (HUVECs) were incubated with growth factor–free medium alone (incomplete medium [IM]) at various concentrations of rGPNMB (25, 50, 100, 250, and 500 ng/ml) for 12 hours. Complete medium (CM), phorbol 12-myristate 13-acetate (PMA; 1 μM), and vascular endothelial growth factor (VEGF; 500 ng/ml) were used as positive controls. Cells were stained with calecin and visualized by fluorescence microscopy. (*B*) Quantitative analysis of the *in vitro* angiogenesis. Values represent means ± SE of three independent experiments. (*C*) For endothelial migration assay, HUVECs were grown to confluence and wounds were made with a pipette tip. The cells were incubated with rGPNMB (500 ng/ml) in the presence or absence of anti-GPNMB antibodies (10 μg/ml) for 24 hours. PMA (1 μM) was used as a positive control. Wound closure index was measured as the distance of the wound closed by rGPNMB. Values are means ± SE of three independent experiments. $^{\#}P < 0.05$ versus anti-GPNMB group; $^{*}P < 0.05$ versus IM group.

Several other targets of miR-150 have been reported. miR-150 can be secreted from human blood cells, and enhances human microvascular endothelial cell migration (32). The migratory effect is mediated by down-regulating v-myc myelocytomatosis viral oncogene homolog (avian) (c-Myb), a potential target of miR-150. c-Myb is a transcription factor that controls lymphocyte development and other cellular functions, including proliferation, apoptosis, and migration (39). miR-150 has also been shown to decrease the tumor-suppressor gene, early growth response-2, thus contributing to the tumorigenic effects in gastric cancer (41). Intraocular injection of pre–miR-150 reduces the VEGF protein level, suggesting that it may be a target of VEGF. However, we did not find any differences in VEGF protein levels in control or hyperoxia-exposed lungs between WT and KO neonates; thus, it is unlikely that VEGF contributes to phenotypic changes of angiogenesis in miR-150 KO neonates.

The loss of VEGF and angiotensin-1 has been linked with impaired vascularity in BPD. A recent study has identified endoglin as an alternative angiogenic factor, which is involved in promoting angiogenesis in long-term ventilated preterm infants (22). GPNMB has been shown to have angiogenic properties (36, 37). Furthermore, induction of GPNMB has been associated with several cancers, where it helps with tumor invasion by reducing apoptosis and promoting endothelial recruitment (42). These studies lead us to speculate as to whether hyperoxia-induced GPNMB in neonatal lungs contributes to angiogenesis or has any protective roles in cellular injury. High induction of lung tissue GPNMB and release of sGPNMB, with prominent increase in capillary network formation in miR-150 KO neonates, support the involvement of GPNMB in angiogenic effects during hyperoxia injury. GPNMB also promoted endothelial tube formation *in vitro* and increased the number of blood vessels formed *in vivo*, providing direct evidence for a role of GPNMB in angiogenesis. The presence of heparin binding domains and RGD domains in the extracellular portion of GPNMB has been attributed to angiogenic effects of GPNMB. RGD binds the β3 class $\alpha_v\beta_3$ integrin on the endothelium and enhances endothelial migration (37). These studies suggest an essential role of GPNMB in promoting endothelial migration and angiogenesis. It would be interesting to further explore whether exogenous administration of GPNMB provokes angiogenesis and helps in the regeneration of alveolar architecture in the injured lungs after hyperoxia exposure.

Interestingly, capillaries formed in KO neonates appeared in an abnormally enlarged size, possibly due to fusion of two or more capillaries. These capillaries were covered with a delicate thin endothelial layer, which was exposed to alveolar air space. Occasionally, the capillaries were also

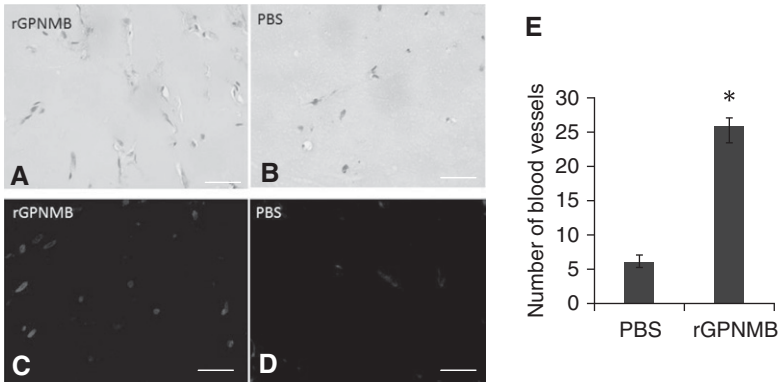


**Figure 7.** *In vivo* matrigel plug assay. An *in vivo* matrigel plug assay was performed to evaluate rGPNMB on angiogenesis. Adult C57BL/6 mice were subcutaneously injected with matrigel containing rGPNMB or PBS. After 14 days, plugs were excised, and sections were stained with hematoxylin and eosin (*A* and *B*) and immunostained with PECAM1 for detection of blood vessels (*C* and *D*). *Scale bars*, 40 μm. Quantitative analysis of blood vessels in matrigel plugs demonstrates a significant increase in the number of blood vessels formed in the presence of rGPNMB (*E*). The experiment was repeated twice ($n = 4$ animals per group). $^*P < 0.001$ versus PBS group.

found beneath the alveolar epithelium, indicating their impairment of the gas exchange function. These vascular abnormalities observed in miR-150 KO neonates have been described before in human neonatal autopsy studies as being due to an increase in endoglin (26). Although these studies linked the abnormal capillaries with lung impairment, we have demonstrated that these changes were reversible when these mice were recovered in room air. We speculate that the capillary abnormalities occur because of earlier damage to the lung alveolar capillary and disruption to the basement membrane. The dysmorphic capillaries were not seen during recovery. Despite abnormality in the lungs during hyperoxia exposure, these neonates do not show signs of fibrosis or abnormal lung growth during their recovery. Moreover, miR-150 KO neonates, which recover faster, have shown an increase in GPNMB-positive cells compared with WT neonates during recovery. These results suggest that an increase in GPNMB may also have an essential role in the recovery of mice after hyperoxia exposure.

Our studies showed more resistance of miR-150 KO neonates to hyperoxia injury than WT neonates after 6 days of exposure, as demonstrated by decreased alveolar and vascular damage. The mechanisms for the resistance in KO neonates are unknown. A recent study has implicated GPNMB in tissue protection by promoting autophagy (40), which induces the autophagy process by directly binding to a microtubule-associated protein 1A/1B–light chain 3/autophagy-related protein 8, thereby enhancing the fusion of an autophagosome with a lysosome. The induction of autophagy further helps in clearing cellular debris, thus reducing inflammation and cellular injury. A recent study has demonstrated the involvement of autophagy in cytoprotection during hyperoxia injury (45). It would be interesting to explore whether GPNMB participates in the hyperoxia-induced autophagy process.

We also found decreased alveolar epithelial apoptosis and cellular infiltrations in miR-150 KO neonates. More inflammation was observed in WT mice, which could be attributed to increased apoptotic cells, which release cytokines/chemokines by activating Fas-mediated signaling during hyperoxia exposure, resulting in an exaggerated inflammatory response (44). Inflammation during BPD has been attributed to the chorioamnionitis caused by infection during gestation. The activation of Toll-like receptor-4 signaling by the early inflammatory response decreases the expression of fibronectin, a basement membrane protein, and thus disrupts epithelial–mesenchymal interaction, leading to the impairment of alveolar growth (43). In the present study, inflammation was observed only on Day 10 of hyperoxia exposure, and alveolar enlargement was prominent even before the onset of cellular infiltration in the lungs of WT neonates. Thus, it is unlikely that alveolar simplification in our animal model is due to inflammation in the lungs.

In conclusion, we report that miR-150 regulation is important in the lung development process during hyperoxia-mediated lung injury. Induced GPNMB during hyperoxia exposure may have a potential role in promoting the angiogenesis process, and thus could provide a potential therapeutic option in reducing lung damage during BPD. ■

**Author disclosures** are available with the text of this article at www.atsjournals.org.

## References

1. Merritt TA, Deming DD, Boynton BR. The 'new' bronchopulmonary dysplasia: challenges and commentary. *Semin Fetal Neonatal Med* 2009;14:345–357.
2. Hayes D Jr, Feola DJ, Murphy BS, Shook LA, Ballard HO. Pathogenesis of bronchopulmonary dysplasia. *Respiration* 2010;79:425–436.
3. Kair LR, Leonard DT, Anderson JM. Bronchopulmonary dysplasia. *Pediatr Rev* 2012;33:255–263.
4. Chess PR, D'Angio CT, Pryhuber GS, Maniscalco WM. Pathogenesis of bronchopulmonary dysplasia. *Semin Perinatol* 2006;30:171–178.
5. Geary C, Caskey M, Fonseca R, Malloy M. Decreased incidence of bronchopulmonary dysplasia after early management changes, including surfactant and nasal continuous positive airway pressure treatment at delivery, lowered oxygen saturation goals, and early amino acid administration: a historical cohort study. *Pediatrics* 2008;121:89–96.
6. Speer CP. Chorioamnionitis, postnatal factors and proinflammatory response in the pathogenetic sequence of bronchopulmonary dysplasia. *Neonatology* 2009;95:353–361.
7. Reininger A, Khalak R, Kendig JW, Ryan RM, Stevens TP, Reubens L, D'Angio CT. Surfactant administration by transient intubation in infants 29 to 35 weeks' gestation with respiratory distress syndrome decreases the likelihood of later mechanical ventilation: a randomized controlled trial. *J Perinatol* 2005;25:703–708.
8. Jobe AH. The new bronchopulmonary dysplasia. *Curr Opin Pediatr* 2011; 23:167–172.
9. Viscardi RM. Perinatal inflammation and lung injury. *Semin Fetal Neonatal Med* 2012;17:30–35.

10. Cerny L, Torday JS, Rehan VK. Prevention and treatment of bronchopulmonary dysplasia: contemporary status and future outlook. *Lung* 2008;186:75–89.
11. Jobe AH, Bancalari E. Bronchopulmonary dysplasia. NICHD/NHLBI/ORD workshop summary. *Am J Respir Crit Care Med* 2001;163:1723–1729.
12. Hayes D Jr, Meadows JT Jr, Murphy BS, Feola DJ, Shook LA, Ballard HO. Pulmonary function outcomes in bronchopulmonary dysplasia through childhood and into adulthood: implications for primary care. *Prim Care Respir J* 2011;20:128–133.
13. Vrijlandt E, Boezen H, Gerritsen J, Stremmelaar E, Duiverman E. Respiratory health inprematurely born preschool children with and without bronchopulmonary dysplasia. *J Pediatr* 2007;150:256–261.
14. Stenmark KR, Abman SH. Lung vascular development: implications for the pathogenesis of bronchopulmonary dysplasia. *Annu Rev Physiol* 2005;67:623–661.
15. Thebaud B, Ladha F, Michelakis ED, Sawicka M, Thurston G, Eaton F, Hashimoto K, Harry G, Haromy A, Korbutt G, *et al*. Vascular endothelial growth factor gene therapy increases survival, promotes lung angiogenesis, and prevents alveolar damage in hyperoxia-induced lung injury: evidence that angiogenesis participates in alveolarization. *Circulation* 2005;112:2477–2486.
16. Abman SH. Bronchopulmonary dysplasia: "a vascular hypothesis." *Am J Respir Crit Care Med* 2001;15:1755–1756.
17. Thébaud B, Abman SH. Bronchopulmonary dysplasia: where have all the vessels gone? Roles of angiogenic growth factors in chronic lung disease. *Am J Respir Crit Care Med* 2007;175:978–985.
18. Jakkula M, LeCras TD, Gebb S, Hirth KP, Tuder RM, Voelkel NF, Abman SH. Inhibition of angiogenesis decreases alveolarization in the developing rat lung. *Am J Physiol Lung Cell Mol Physiol* 2000; 279:L600–L607.
19. Klekamp JG, Jarzecka K, Perkett EA. Exposure to hyperoxia decreases the expression of vascular endothelial growth factor and its receptors in adult rat lungs. *Am J Pathol* 1999;154:823–831.
20. Maniscalco WM, Watkins RH, Pryhuber GS, Bhatt A, Shea C, Huyck H. Angiogenic factors and alveolar vasculature: development and alterations by injury in very premature baboons. *Am J Physiol Lung Cell Mol Physiol* 2002;282:L811–L823.
21. Maeda Y, Dave V, Whitsett JA. Transcriptional control of lung morphogenesis. *Physiol Rev* 2007;87:219–244.
22. Bhatt AJ, Pryhuber GS, Huyck H, Watkins RH, Metlay LA, Maniscalco WM. Disrupted pulmonary vasculature and decreased vascular endothelial growth factor, Flt-1, and TIE-2 in human infants dying with bronchopulmonary dysplasia. *Am J Respir Crit Care Med* 2001; 164:1971–1980.
23. Fukumura D, Gohongi T, Kadambi A, Izumi Y, Ang J, Yun CO, Buerk DG, Huang PL, Jain RK. Predominant role of endothelial nitric oxide synthase in vascular endothelial growth factor–induced angiogenesis and vascular permeability. *Proc Natl Acad Sci USA* 2001;98: 2604–2609.
24. Kunig AM, Balasubramaniam V, Markham NE, Morgan D, Montgomery G, Grover TR, Abman SH. Recombinant human VEGF treatment enhances alveolarization after hyperoxic lung injury in neonatal rats. *Am J Physiol Lung Cell Mol Physiol* 2005;289:L529–L535.
25. D'Angio CT, Maniscalco WM. The role of vascular growth factors in hyperoxia-induced injury to the developing lung. *Front Biosci* 2002;7: d1609–d1623.
26. De Paepe ME, Patel C, Tsai A, Gundavarapu S, Mao Q. Endoglin (CD105) up-regulation in pulmonary microvasculature of ventilated preterm infants. *Am J Respir Crit Care Med* 2008;178:180–187.
27. Cherni I, Weiss GJ. miRNAs in lung cancer: large roles for small players. *Future Oncol* 2011;7:1045–1055.
28. Tomankova T, Petrek M, Kriegova E. Involvement of microRNAs in physiological and pathological processes in the lung. *Respir Res* 2010;11:159.
29. Wang Y, Stricker HM, Gou D, Liu L. MicroRNA: past and present. *Front Biosci* 2007;12:2316–2329.
30. Shen J, Yang X, Xie B, Chen Y, Swaim M, Hackett SF, Campochiaro PA. MicroRNAs regulate ocular neovascularization. *Mol Ther* 2008; 16:1208–1216.
31. Poliseno L, Tuccoli A, Mariani L, Evangelista M, Citti L, Woods K, Mercatanti A, Hammond S, Rainaldi G. MicroRNAs modulate the angiogenic properties of HUVECs. *Blood* 2006;108:3068–3071.
32. Zhang Y, Liu D, Chen X, Li J, Li L, Bian Z, Sun F, Lu J, Yin Y, Cai X, *et al*. Secreted monocytic miR-150 enhances targeted endothelial cell migration. *Mol Cell* 2010;39:133–144.
33. Yamasaki K, Nakasa T, Miyaki S, Yamasaki T, Yasunaga Y, Ochi M. Angiogenic microRNA-210 is present in cells surrounding osteonecrosis. *J Orthop Res* 2012;30:1263–1270.
34. Bhaskaran M, Xi D, Wang Y, Huang C, Narasaraju T, Shu W, Zhao C, Xiao X, More S, Breshears M, *et al*. Identification of microRNAs changed in the neonatal lungs in response to hyperoxia exposure. *Physiol Genomics* 2012;44:970–980.
35. Sheng MH, Wergedal JE, Mohan S, Lau KH. Osteoactivin is a novel osteoclastic protein and plays a key role in osteoclast differentiation and activity. *FEBS Lett* 2008;582:1451–1458.
36. Rose AA, Annis MG, Dong Z, Pepin F, Hallett M, Park M, Siegel PM. ADAM10 releases a soluble form of the GPNMB/Osteoactivin extracellular domain with angiogenic properties. *PLoS One* 2010;5: e12093.
37. Reynolds AR, Hart IR, Watson AR, Welti JC, Silva RG, Robinson SD, Da VG, Gourlaouen M, Salih M, Jones MC, *et al*. Stimulation of tumor growth and angiogenesis by low concentrations of RGD-mimetic integrin inhibitors. *Nat Med* 2009;15:392–400.
38. Bhaskaran M, Wang Y, Zhang H, Weng T, Baviskar P, Guo Y, Gou D, Liu L. MicroRNA-127 modulates fetal lung development. *Physiol Genomics* 2009;37:268–278.
39. Xiao C, Calado DP, Galler G, Thai TH, Patterson HC, Wang J, Rajewsky N, Bender TP, Rajewsky K. MiR-150 controls B cell differentiation by targeting the transcription factor c-Myb. *Cell* 2007;131:146–159.
40. Li B, Castano AP, Hudson TE, Nowlin BT, Lin SL, Bonventre JV, Swanson KD, Duffield JS. The melanoma-associated transmembrane glycoprotein GPNMB controls trafficking of cellular debris for degradation and is essential for tissue repair. *FASEB J* 2010;24:4767–4781.
41. Wu Q, Jin H, Yang Z, Luo G, Lu Y, Li K, Ren G, Su T, Pan Y, Feng B, *et al*. MiR-150 promotes gastric cancer proliferation by negatively regulating the pro-apoptotic gene EGR2. *Biochem Biophys Res Commun* 2010;392:340–345.
42. Kuan CT, Wakiya K, Dowell JM, Herndon JE II, Reardon DA, Graner MW, Riggins GJ, Wikstrand CJ, Bigner DD. Glycoprotein nonmetastatic melanoma protein B, a potential molecular therapeutic target in patients with glioblastoma multiforme. *Clin Cancer Res* 2006;12:1970–1982.
43. Prince LS, Dieperink HI, Okoh VO, Fierro-Perez GA, Lallone RL. Toll-like receptor signaling inhibits structural development of the distal fetal mouse lung. *Dev Dyn* 2005;233:553–561.
44. De Paepe ME, Mao Q, Chao Y, Powell JL, Rubin LP, Sharma S. Hyperoxia-induced apoptosis and Fas/FasL expression in lung epithelial cells. *Am J Physiol Lung Cell Mol Physiol* 2005;289:L647–L659.
45. Tanaka A, Jin Y, Lee SJ, Zhang M, Kim HP, Stolz DB, Ryter SW, Choi AM. Hyperoxia-induced LC3B interacts with the Fas apoptotic pathway in epithelial cell death. *Am J Respir Cell Mol Biol* 2012;46:507–514.